2020 IMEKO TC-19 International Workshop on
Metrology for the Sea
Naples, Italy, October 5-7, 2020

Tsunamigenic mass-failure scenarios in the Palinuro volcano chain

Glauco Gallotti[1], Guido Ventura[2], Alberto Armigliato[1], Filippo Zaniboni[1], Gianluca Pagnoni[1], Liang Wang[1], Salvatore Passaro[3], Marco Sacchi[3], Marco Ligi[3], Stefano Tinti[1]

[1] *University of Bologna, Department of Physics and Astronomy (DIFA), Bologna, Italy.* (glauco.gallotti2@unibo.it)
[2] *National Institute of Geophysics and Volcanology (INGV), Roma, Italy.*

[3]*Institute of Marine Sciences (ISMAR), National Research Council (CNR), Napoli, Italy.*

***Abstract* –The Palinuro volcanic chain is located nearly 80 km offshore the Campania coasts (Italy), in the southern sector of the Tyrrhenian Sea. 15 distinct volcanic edifices have been recently detected. The presence of shallow seismicity and active hydrothermal activity suggests that this large volcanic chain is still active. Specific sectors of the complex show the existence of ongoing slope instability. Thus, the chance of mass movements following seismic or volcanic activity cannot be ruled out. Stability analysis for typical seismic loads in such a volcanic area has been performed. Three mass failure scenarios have been reconstructed through numerical models in the weaker sections found. The tsunami triggered by each slide has been simulated, and large waves have been found in two of the three hypothesized scenarios. For the biggest slide of 2.4 km^3, waves as high as 6 m could reach portions of the Calabria region coasts.**

I. INTRODUCTION

Morphological evidence of flank and sector collapses are a common feature of volcanic structures ([1], [2], [3]). Several factors are responsible for the weakening mechanisms at volcanoes and consequent instability. Namely: magmatic upraise or withdrawal, hydrothermal processes, volcano-tectonics, earthquakes, and climate factors ([4], [5]). In the case of volcanic islands and seamounts, gravity instability events can lead to the generation of tsunami waves. These waves can travel hundreds of kilometers in a short time [6]. As opposed to the tsunamis associated with earthquakes, tsunamis related to volcano instability typically show shorter-period waves and, with few exceptions (e.g., the 1883 Krakatau tsunami) produce less devastating far-field damages [7]. In the Tyrrhenian Sea, the most recent event of this kind took place in December 2002 at Stromboli Island, Italy, and involved the submarine and subaerial sectors of the volcano. A maximum wave run-up of $8\,m$ has been detected along the coast of Stromboli [8]. The study of the instability of seamounts is fundamental to estimate (1) the coastal exposition to this kind of hazard, and (2) the impact on population and infrastructures. The Palinuro Volcanic Chain (PVC) is located in the Southern Tyrrhenian Sea (Italy, see Fig. 1). This is a 2 Ma old back-arc basin associated with the north-westward subduction of the Ionian Sea below the Calabrian Arc [9]. The Tyrrhenian back-arc includes 33 known volcanic seamounts [10], mostly concentrated in the submerged portion of the Aeolian volcanic Arc. The about 70 km long PVC emplaces along with an E-W striking strike-slip fault system. It consists of 15 E-W aligned volcanoes with height up to 3200 m from the seafloor [11]. The presence of calderas (to the west), slide scars, and incised canyons provide evidence of instability phenomena [12].

Northern and southern flanks of the PVC ridge have asymmetric slopes, both characterized by canyons and slide scars that rule the sediment displacement. The northern flank has an average slope of $18°$ and the erosional base level is located at $-1600\,m$ below the sea level (Palinuro Basin), while the southern flank of the PVC shows $20° - 30°$ slope values and reaches ca. $-3200\,m$ depth, where it drastically changes to $2°$ slope that characterizes the northernmost sector of the Marsili Basin. Furthermore, the occurrence of hydrothermal and seismic activity (both shallow and deep) suggests that instability events cannot be ruled out ([13], [14]).

To investigate this aspect, this study performs a stability analysis of specific sectors of the PVC. Eventually, mass failures and consequent tsunami generations are evaluated in the weakest sections found.

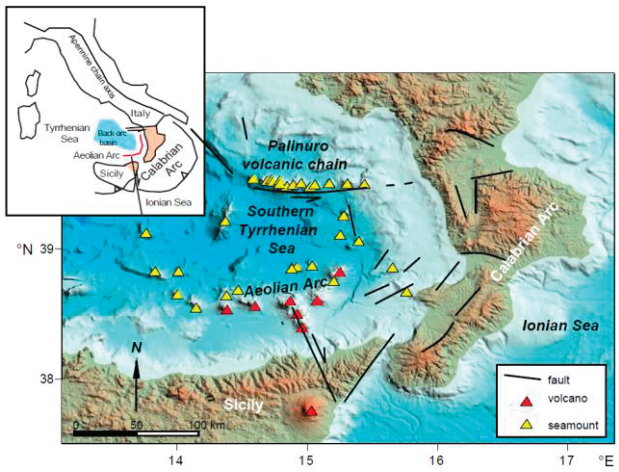

Fig. 1. The Southern Tyrrhenian Sea basin. Seamounts and volcanoes are shown with yellow and red triangles, respectively.

II. DATA AND MODELING

A detailed Digital Terrain Model (DTM) of the upper part of the PVC and a seismic profile have been used to locate the areas objects of the stability analysis. Multibeam data acquisition was carried out in the frame of the "Aeolian_2007" oceanographic cruise onboard the Urania oceanographic vessel by the National Research Council (CNR). Data were collected by using the Reason Seabat 8160 multibeam sonar system, suitable for $50-3500\,m$ depth range data acquisition. The equipment was characterized by a ping source of $50\,kHz, 150°$ for the whole opening of the transmitted pulse, and a 126 beams-receiver. Sound velocity profiles were acquired and real-time applied for beam pattern calibration every 6-8 hours during the survey. The final DTM (see Fig. 3) was obtained after tidal correction and de-spiking by using PDS2000 grid tools and shows ca. $1000\,km2$ of seafloor morphologies (min/max depth are $-84\,m/-1200\,m$). The migrated multichannel seismic line TYR10_12 has been acquired during the 2010 TIR10 cruise, perpendicular to the chain direction. Technical details are reported in [15].

In this work, analysis and simulations have been performed employing a set of numerical models. This procedure has been applied to reproduce landslides or landslides-tsunami events [16], [17], [18]. The stability analysis to determine the sectors associated with potential mass movements is carried out through a numerical code implementing the minimum lithostatic deviation (MLD) method [19]. This is a 2D revised technique of the classic limit-equilibrium method (LEM). The outputs of the stability analysis allow the identification of potential initial sliding areas. Thus, the slides' motion is computed employing two numerical models: UBO-BLOCK2 [20] and UBO-DAF [21]. Eventually, the code UBO-TSUIMP and the numerical code UBO-TSUFD simulate the wave generation and propagation, respectively (for more details, see [22]).

The adopted regular computational grids for both landslide models are $50\,m$ spaced, obtained starting from the EMODnet database (2018). The finer grid ($25\,m$ spaced) embracing merely the seamounts' superior sections has been used for the stability analysis. The UBO-TSUIMP model runs on a $250\,m$ regularly spaced domain, obtained by interpolating ~~of~~ the above-mentioned EMODnet dataset. Eventually, the tsunami propagation is computed over a $750\,m$ spaced grid, covering the whole Tyrrhenian Basin.

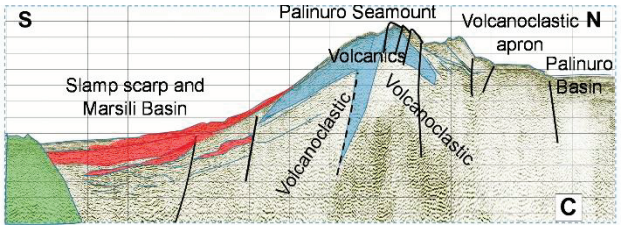

Fig. 2. Modified TYR10_12 multi-channel seismic profile.

III. RESULTS

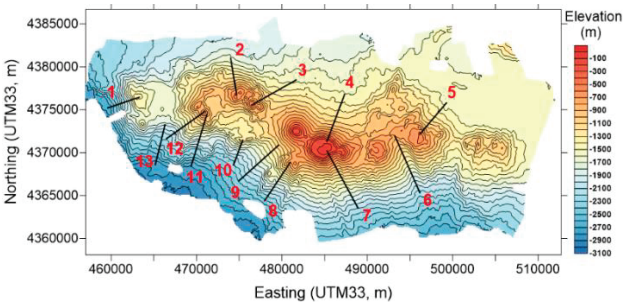

Fig. 3. Selected profiles for the stability analysis. Datum is WGS84.

A. Stability analysis

As many as 13 profiles have been selected for the stability analysis (Fig. 3). The above-mentioned seismic line TYR10_12 is located near profile 7. The other profiles are located in similar canyons throughout the seamount. The analysis is carried out without considering the seismic load induced by tectonic earthquakes. Due to the considerable distance from the volcanic chain ($> 200\,km$), even the strongest historical tectonic earthquakes of the surrounding regions cannot produce evident effects. Controversially, shallow ($< 5\,km$) volcanic earthquakes ($3.6 < M < 4.8$) can generate relevant local Peak Ground Accelerations (PGAs). These are estimated through a relationship calibrated over an Etna seismic sequence (see [23] for details). Specifically, two reference distances ($r_1 = 1\,km,\ r_2 = 5\,km$) and two typical volcanic soils are considered. Results have shown that PGAs as high as 0.15

can be expected in the surroundings of the profiles. The stability analysis eventually requires a series of inputs in terms of geotechnical parameters (i.e. friction angle ϕ, cohesion c, and rock unit weight γ). Due to the lack of specific information about the slopes' characteristics, four sets of the above-mentioned parameters have been properly selected (Table 1), following considerations in other studies (see [2], [24], [25]). Results have proved that profiles 1, 7, 11, and 12 can be potentially destabilized, especially for set s_2 and PGA >0.05-0.1. Due to the proximity of profiles 11 and 12, only one scenario has been reconstructed in this sector.

Table 1. Selected geotechnical parameters for the stability analysis.

Set	$\boldsymbol{\phi}$ (°)	$\boldsymbol{c}$ $(\boldsymbol{kPa})$	$\boldsymbol{\gamma}$ $(\boldsymbol{kN/m^3})$
s_1	30	5	20
s_2	30	5	15
s_3	33	5	20
s_4	33	5	15

B. Mass Failures

Mass failure scenarios have been reconstructed in the weakest sectors of the PVC, following the stability analysis results. The sliding volumes reconstruction is based on the local geomorphological features and the information gathered from the seismic profile. Pointedly, the hypothesized sliding volumes involve different orders of magnitude to evaluate the related scale of the triggered tsunami. Pointedly, the slide volumes are $0.7\ Mm^3, 1.5\ km^3, 2.4\ km^3$ for P1, P2, and P3, respectively. A basal friction coefficient $\mu = 0.05$ is assumed, considering a set of landslide parameters adopted by [26] in a similar environment. The results of both models have shown the slides reach maximum velocities in the order of $60\ m/s$. The accelerating phase of the motion (the most important for the tsunami generation) is performed by both models similarly.

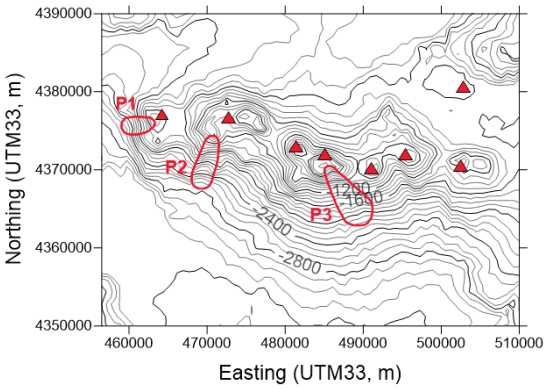

Figure 4. Initial sliding areas for the simulated mass failures, bounded by red lines. Red triangles show the volcanic vents.

C. Tsunami generation and propagation

The three reconstructed mass failures generate three distinct tsunamis waves. Their amplitude is different due to the different depths and sliding volumes. We have studied their radiation in the basin's central and southern parts, where the waves are larger. In the panels of Fig. 5, the maximum and minimum water elevation in the basin for the first 2-hrs propagation time are shown. The P1 scenario involves small elevations. This implies the generation of a tsunami wave not relevant in terms of hazards. What is of interest here, are the P2 and P3 scenarios, where maximum water elevations found are in the order of meters. Maxima and minima are not symmetrically distributed around zero. Close to the source, troughs extent prevail on the crests. Far from it, differences tend to reduce, but minima have a slightly larger magnitude than maxima, with some exception.

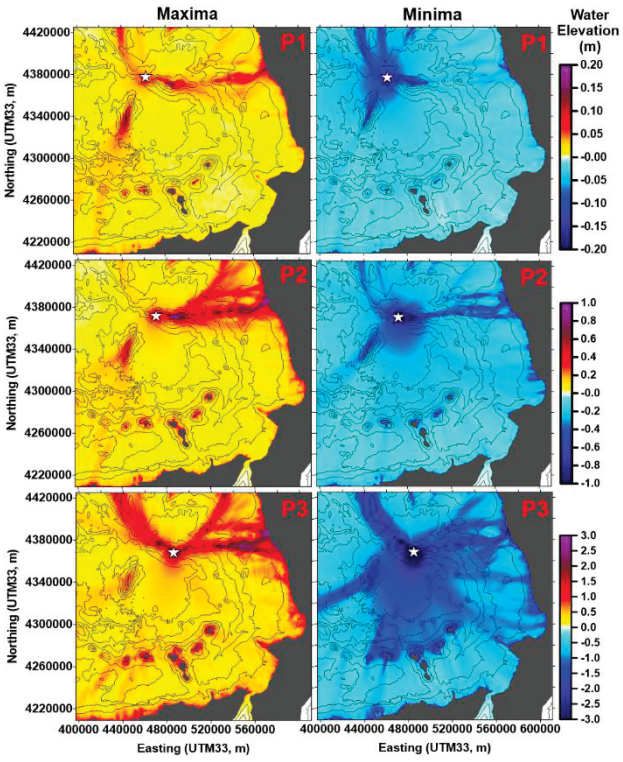

Figure 5. Maximum (left panels) and minimum (right panels) water elevations in the P1, P2, and P3 scenarios over the south-eastern sector of the Tyrrhenian sea. The white stars denote the initial sliding areas. Note that the palette saturates at different values in the three cases.

The tsunami propagation pattern is far from being isotropic. It is characterized by a strong concentration of tsunami energy along with some preferential patterns. This depends on the tsunami sources, but mostly on the bathymetry that

influences the waves' phase velocity. Given the above considerations, the tsunami propagations have been studied for the P2 and P3 cases. Results are shown in Fig. 6 in field snapshots taken at six instants from 1 to 30 *min*. Tsunami positive leading front is found along the direction of the landslide motion, and the negative one in the opposite direction. Also, the propagation patterns are similar, showing the initial radial spreading typical of landslide-tsunamis.

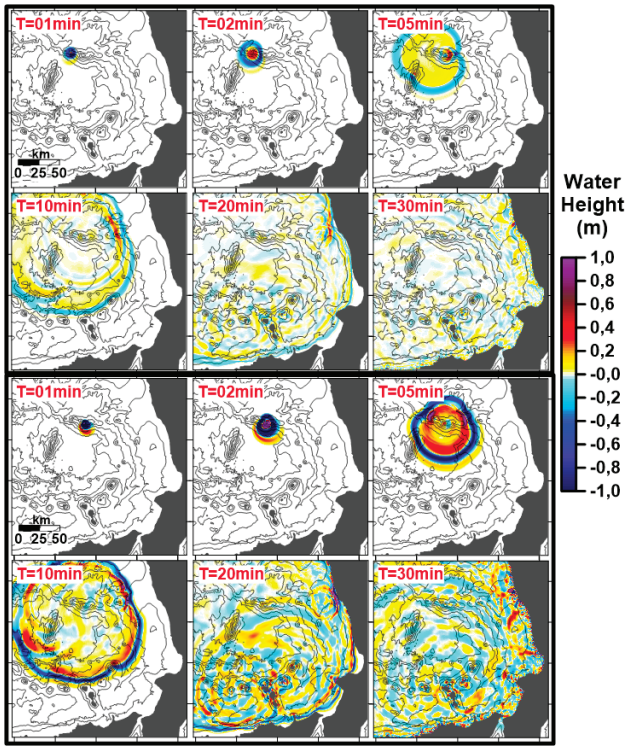

Figure 6. Sea elevations fields for the P2 (upper panels) and P3 (lower panels) scenarios in the Southern Tyrrhenian Sea.

For the sake of brevity, we do not show the tsunami elevation along the coasts. Results proved that, for P2 case, the eastern coasts of the basin (from Campania to Calabria) are affected by waves generally around $0.5\,m$, the southern coasts (Sicily) by waves around $0.4\,m$ and the western coast (Sardinia) by waves around $0.2\,m$. As for the amplitudes, the peak around $1.5\,m$ is found in northern Calabria. For P3 scenario, the tsunami amplitudes are much higher. Wave height is around $2-2.5\,m$ on the eastern coast, around $2\,m$ on Sicily, and around $0.4-0.6\,m$ on Sardinia. The peak is found in the same location as P2 and it is as high as $6\,m$. Further, two more peaks are worth of notice: one around $4\,m$ at Vaticano Cape (southern Calabria) and the other with an elevation of nearly $3\,m$ at Mondello Cape, to the west of Palermo, Sicily.

IV. DISCUSSION AND CONCLUSIONS

This study has evaluated the effects of the possible occurrence of mass failures on the flanks of the PVC. To this goal, a preliminary stability analysis has been carried out. Typical volcanic soils and PGAs induced by shallow volcanic earthquakes have been considered. Results proved that 30% of the selected profiles could be destabilized as a consequence of moderate volcanic earthquakes ($3.6 < M < 4.8$). In other studies, concerning similar locations, stronger earthquakes have been considered (e.g. [27]). Also, the four sets of geotechnical parameters do not consider the possible alterations of rocks related to the hydrothermal activity. Thus, the results of this analysis could be slightly underestimated.

We have imposed the mass failures characteristics based on the available information. Simulations show similar results, especially in the accelerating phase of the motion. The three different-size slides scenarios allowed us to study the relationship between sliding volumes, depth, and size of the generated tsunamis at PVC. The sliding volumes being correlated to the size of the tsunamis, and anti-correlated with depths (as can be expected in the case of rockslides). Two scenarios (P2 and P3) show sea surface elevations in the order of $1\,m$ and $5\,m$, respectively. Of note is the presence of bent paths (beams) where maximum and minimum water elevations are found, also covering the PVC summits. Furthermore, the elevation along the coasts proved that maxima are found for both scenarios in the same location (northern Calabria region). These values are in the order of $1.5\,m$ and $6\,m$, respectively, and then potentially hazardous. Further details about this aspect and the whole study can be found in [28].

These results highlight the need for more detailed studies and oceanographic cruises to reveal the nature and characteristics of the PVC and the other abundant Tyrrhenian seamounts. This information would allow the reconstruction of more exhaustive scenarios to assess a landslide-induced tsunami hazard for the Tyrrhenian coasts properly.

V. REFERENCES

[1] W.J. McGuire, "Volcano instability: a review of contemporary themes." Geological Society, London, Special Publications, 110, 1-23, 1996. https://doi.org/10.1144/GSL.SP.1996.110.01.01.

[2] T. Apuani, C. Corazzato, "Etna flank dynamics: A sensitivity analysis by numerical modelling." In C. Olalla, L.E. Hernandez, J.A. Rodriguez-Losada, J. Gonzalez-Gallego (Eds.), "Volcanic rock mechanics — rock mechanics and geo-engineering in volcanic environments", Papers from the 3rd ISRM

International Workshop, Puerto de la Cruz, Tenerife (Canary Islands), Spain, 31 May–1 June 2010, 978-0-415-58478-4, Taylor & Francis Group, London, pp. 151-157, 2010.

[3] J.C. Thouret, "Volcanic hazards and risks: a geomorphological perspective." in Geomorphological Hazards and Disaster Prevention, e.I.A.-A.a.A.S. Goudie, Editor. Cambridge University Press, pp. 13-32, 2010.

[4] M.E. Reid, T.W. Sisson, D.L. Brien, "Volcano collapse promoted by hydrothermal alteration and edifice shape, Mount Rainer, Washington." Geology, 79: 779-782, 2010.

[5] B. van Wyk de Vries, A. Delcamp, "Volcanicdebris avalanches." In: Davies T (Editor) "Landslide hazards, risks, and disasters." Elsevier, Amsterdam, pp. 131-153, 2016.

[6] R. Paris, "Source mechanisms of volcanic tsunamis." Phil. Trans. R. Soc. A, 373: 20140380, 2015. http://dx.doi.org/10.1098/rsta.2014.0380.

[7] C.B. Harbitz, F. Løvholt,, G. Pedersen, D.G. Masson, "Mechanisms of tsunami generation by submarine landslides: a short review." Norwegian J. Geol., 86:255-264, 2006.

[8] A. Maramai, L. Graziani, G. Alessio, P. Burrato, L. Colini, L. Cucci, R. Nappi, A. Nardi, G. Vilardo, "Near- and far-field survey report of the 30 December 2002 Stromboli Southern Italy tsunami." Mar. Geol., 215: 93-106, 2005. https://doi:10.1016/j.margeo.2004.11.009.

[9] C. Faccenna, F. Funiciello, L. Civetta, L., M.D. Antonio, M. Moroni, C. Piromallo, "Slab disruption, mantle circulation, and the opening of the Tyrrhenian basins." In "Cenozoic Volcanism in the Mediterranean Area" (Eds. Beccaluva, L., Bianchini, G., Wilson, M.), Geol. Soc. America Special Paper 418, pp. 153-169, 2007.

[10] A. Pensa, A. Pinton, L. Vita, A. Bonamico, A.A. De Benedetti, G. Giordano "ATLAS of Italian Submarine Volcanic Structures." Memorie Descrittive della Carta Geologica d'Italia, 104: 77- 183, 2019.

[11] L. Cocchi, S. Passaro, F.C. Tontini, G. Ventura "Volcanism in slab tear faults is larger than in island-arcs and back-arcs." Nature Commun. 8: 1451, 2017. https://doi.org/10.1038/s41467-017-01626-w.

[12] S. Passaro, G. Milano, C. D'Isanto, S. Ruggieri, R. Tonielli, P.P. Bruno, M. Sprovieri, E. Marsella, E. "DTM-based morphometry of the Palinuro seamount (Eastern Tyrrhenian Sea): Geomorphological and volcanological implications." Geomorphology, 115: 129-140, 2010. doi:10.1016/j.geomorph.2009.09.041.

[13] F.C. Tontini, G. Bortoluzzi, C. Carmisciano, L. Cocchi, C. de Ronde, M. Ligi, F. Muccini, "Near-Bottom Magnetic Signatures of Submarine Hydrothermal Systems at Marsili and Palinuro Volcanoes, Southern Tyrrhenian Sea, Italy." Economic Geology, 109: 2119-2128, 2014.

[14] A. Rovida, M. Locati, R. Camassi, B. Lolli, P. Gasperini, "Catalogo Parametrico dei Terremoti Italiani (CPTI15), versione 2.0." Istituto Nazionale di Geofisica e Vulcanologia (INGV), 2019. https://doi.org/10.13127/CPTI/CPTI15.2.

[15] M. Ligi, L. Cocchi, G. Bortoluzzi, F. D'Oriano, F., Muccini, F.C. Tontini, C.E.J. De Ronde, C. Carmisciano, "Mapping of seafloor hydrothermally altered rocks using geophysical methods: Marsili and Palinuro seamounts, southern Tyrrhenian Sea." Economic Geology, 109: 2103-2117, 2014.

[16] F. Zaniboni, G. Pagnoni, S. Tinti, M. Della Seta, P. Fredi, E. Marotta, G. Orsi, "The potential failure of Monte Nuovo at Ischia Island (Southern Italy): numerical assessment of a likely induced tsunami and its effects on a densely inhabited area." Bull. Volcanol., 75: 763, 2013. doi:10.1007/s00445-013-0763-9.

[17] F. Zaniboni, S. Tinti, "The 1963 Vajont landslide: a numerical investigation on the sliding surface heterogeneity." Pure Appl. Geophys., 176: 279-295, 2019. https://doi.org/10.1007/s00024-018-2023-6.

[18] F. Zaniboni, G. Pagnoni, G. Gallotti, M.A. Paparo, A. Armigliato, S. Tinti, "Assessment of the 1783 Scilla landslide-tsunami's effects on the Calabrian and Sicilian coasts through numerical modelling." Nat. Hazards Earth Syst. Sci., 19, 1585–1600, 2019. https://doi.org/10.5194/nhess-19-1585-2019.

[19] S. Tinti, A. Manucci, "Gravitational stability computed through the limit equilibrium method revisited." Geophys. J. International, 164: 1-14, 2006.

[20] S. Tinti, S., Bortolucci, E., Vannini, C. "A block-based theoretical model suited to gravitational sliding." Nat. Hazards, 16: 1-28, 1997.

[21] L. Wang, F. Zaniboni, S. Tinti, X. Zhang "Reconstruction of the 1783 Scilla landslide, Italy: numerical investigations on the flow-like behaviour of landslides." Landslides, 16: 1065-1076, 2019.

[22] S. Tinti, R. Tonini "The UBO-TSUFD tsunami inundation model: validation and application to a tsunami case study focused on the city of Catania, Italy." Nat. Hazards Earth Syst. Sci., 13: 1795-1816, 2013. https://doi.org/10.5194/nhess-13-1795-2013.

[23] G. Tusa, H. Langer "Prediction of ground motion parameters for the volcanic area of Mount Etna." J. Seismol., 20: 1-42, 2016. https://doi10.1007/s10950-015-9508-x.

[24] L.N., Schaefer, T. Oommen, C. Corazzato, A. Tibaldi, R.I. Escobar-Wolf, W. Rose, "An integrated field-numerical approach to assess slope stability hazards at volcanoes: the example of Pacaya, Guatemala." Bull.Volcanol., 75:720, 2013. https://doi:10.1007/s00445-013-0720-7

[25] C.E. Harnett, J.E. Kendrick, A. Lamur, M.E. Thomas, A. Stinton, P.A. Wallace, J.E.P. Utley, W. Murphy, J.

Neuberg, Y. Lavallée, “Evolution of Mechanical Properties of Lava Dome Rocks Across the 1995–2010 Eruption of Soufrière Hills Volcano, Montserrat.” Front. Earth Sci., 7: 7, 2019. https://doi.org/10.3389/feart.2019.00007.

[26] K. Kelfoun, T. Giachetti, P. Labazuy, “Landslide‐generated tsunamis at Rèunion Island.” J. Geophys. Res., 115: F04012, 2010. https://doi:10.1029/2009JF001381.

[27] R. del Potro, M. Hürlimann, H. Pinkerton, “Modelling flank instabilities on stratovolcanoes: Parameter sensitivity and stability analyses of Teide, Tenerife.” J. Vol. Geotherm. Res., 256: 50-60, 2013.

[28] G. Gallotti, S. Passaro, A. Armigliato, F. Zaniboni, G. Pagnoni, L. Wang, M. Sacchi, S. Tinti, “Potential mass movements on the Palinuro volcanic chain (southern Tyrrhenian Sea, Italy) and consequent tsunami generation.”J. Volcanol. Geotherm. Res., 404: 107025, 2020. https://doi.org/10.1016/j.jvolgeores.2020.107025.